ISSN 1062-8738, Bulletin of the Russian Academy of Sciences: Physics, 2019, Vol. 83, No. 7, pp. 828–831. © Allerton Press, Inc., 2019.
Russian Text © The Author(s), 2019, published in Izvestiya Rossiiskoi Akademii Nauk, Seriya Fizicheskaya, 2019, Vol. 83, No. 7, pp. 910–913.

Resonant Spin Pumping in an Acoustic Microwave Resonator with ZnO-GGG-YIG/Pt Structure

N. I. Polzikova[a], *, S. G. Alekseev[a], V. A. Luzanov[b], and A. O. Raevskiy[b]

[a] *Kotelnikov Institute of Radio Engineering and Electronics, Russian Academy of Sciences, Moscow, 125009 Russia*
[b] *Kotelnikov Institute of Radio Engineering and Electronics, Fryazino Branch, Russian Academy of Sciences, Fryazino, Moscow oblast, 141190 Russia*
**e-mail: polz@cplire.ru*

Received September 7, 2018; revised January 31, 2019; accepted March 27, 2019

Abstract—A theory of acoustic spin pumping in a bulk acoustic wave resonator with a ZnO-YIG-GGG-YIG/Pt structure is presented, with allowance for the exchange contribution to the formation of a coupled magnetoelastic wave spectrum, and the back action of acoustically excited magnetic dynamics in YIG films on the elastic subsystem in all layers. Good agreement is achieved between the theoretical and experimental frequency–field dependences of the resonant frequencies of the resonator and the voltage magnitude of the inverse spin Hall effect in Pt.

DOI: 10.3103/S1062873819070323

In magnetoelectric composite structures containing piezoelectric or ferro(ferri)magnetic (FM) layers, ferromagnetic resonance (FMR) or acoustically driven spin waves (ADSWs) can be excited under the action of an alternating electric field, due to the piezoeffect or to the magnetostriction in corresponding layers. Since such electroacoustic excitation of spin dynamics does not require the use of alternating magnetic fields or the currents that induce them, ADSW-based devices can operate with low energy consumption. ADSWs are promising in particular for use in microwave spintronics to generate acoustic spin pumping (ASP), i.e., transformation of the spin angular momentum of ADSWs into direct spin current (SC) at FM–non-magnetic metal interfaces [1–3].

In [4, 5], we proposed using an magnetoelectric spintronic resonator of bulk acoustic waves (AWs) with the structure of yttrium iron garnet (YIG)/Pt to create an effective ASP (Fig. 1). In gigahertz frequency range f, film piezotransducer *2-1-2* generates high resonator modes f_n ($n \sim 500$) with intermode distance $\Delta f_n \sim 2$–3 MHz [6]. In magnetic field $\vec{H}$ corresponding to the magnetoelastic resonance (MER), the accumulated elastic energy is effectively transmitted into a magnetic subsystem, which generates ADSWs in YIG films *3*, *5*. As was shown in [7–9], frequencies $f_n(H)$ are shifted and split by the field change in the vicinity of the MER, which is a consequence of the ADSW back action on the elastic subsystem of all layers. The variation of the frequency dependence of reflection coefficient S_{11} under the action of the magnetic field thus allows indirect detection of ADSWs using the piezotransducer.

Another way of electrical detection of ADSWs is to measure the direct voltage in a nonmagnetic metal in

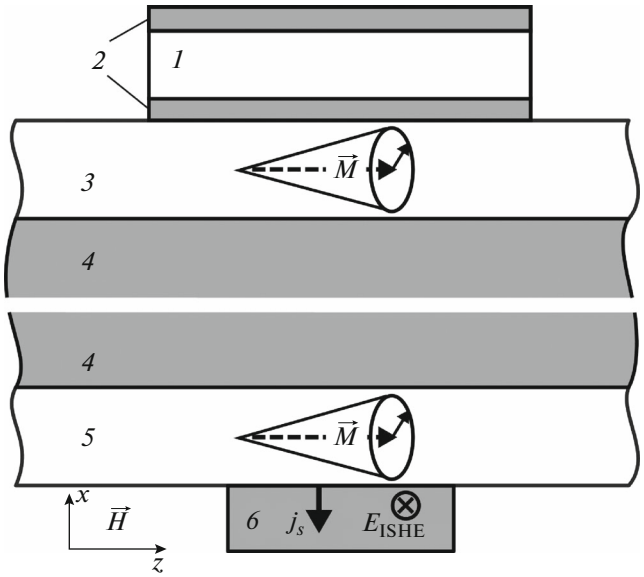

Fig. 1. Resonator scheme: (*1*) ZnO film; (*2*) Al electrodes 0.15–0.2 μm thick, with diameters of a = 170 μm in the overlap region; (*3, 5*) epitaxial YIG films; (*4*) GGG single-crystal substrate; (*6*) thin Pt film formed as a stripe directed normal to the plane of the structure. Direct electric field $\vec{E}_{\text{ISHE}}$ generates electric voltage $U_{\text{ISHE}} = (\vec{E}_{\text{ISHE}}\vec{a})$.

contact with an FM. At the interface between the YIG and the nonmagnetic metal (Pt), the spin angular momentum of an ADSW is transformed into direct SC $\vec{j}_s$; i.e., spin pumping is generated [10]. The SC is detected as a result of its transformation into conduction current, due to the inverse spin Hall effect (ISHE) [11]. Measuring direct voltage U_{ISHE} at the Pt stripe ends thus allows direct detection of ADSWs and the SCs generated by them.

Using simultaneous frequency–field scanning of reflection coefficient S_{11} and voltage U_{ISHE} in [5], we detected considerable asymmetry in the behavior of $U_{\text{ISHE}}(f, H)$ with respect to the MER frequency, which is not observed in dependence $S_{11}(f, H)$. This is a reflection of the qualitative difference between the above characteristics of ADSWs. Dependence $S_{11}(f, H)$ is an indirect and integral characteristic that reflects variations in the phase incursions of AWs over the thickness of an FM layer as a result of the change in dispersion characteristics and the corresponding phase velocity in the MER range. Dependence $U_{\text{ISHE}}(f, H)$ contains information about the precession of magnetization directly at the FM/Pt interface.

In this work, we develop a theoretical model describing the generation of ADSWs and SC in the YIG/Pt system using a piezoelectric transducer under the conditions of double resonance: the MER in the YIG film and the pure elastic resonance throughout the multi-layer structure of the AW resonator. This model considers the contribution from nonuniform exchange to the forming of the coupled magnetoelastic wave spectra in the YIG films, the corresponding boundary conditions, and the characteristics of the resonator's piezoelectric excitation. The results of $U_{\text{ISHE}}(f, H)$ and $S_{11}(f, H)$ calculation allow us to obtain qualitative and quantitative agreement with the experimental data. The effect the YIG film thickness on the above dependences is considered.

We use linear and one-dimensional approximations, assuming that all variables depend on coordinate x and time t as $\exp[i(k^{(j)}x - 2\pi ft)]$, where $k^{(j)}$ is the wavenumber in the j-th layer. In nonmagnetic layers, solving the wave equations for elastic displacements $u_z^{(j)}$ yields relation $k^{(j)} = \pm(2\pi f/V^{(j)})$, where $V^{(j)} = \sqrt{C^{(j)}/\rho^{(j)}}$ is the phase velocity of a shear AW in a medium with density $\rho^{(j)}$ and elastic modulus $C^{(j)}$. In FM layers (superscripts $j = 3, 5$ are omitted below), we consider the magnetoelastic contribution to the energy density, which results in coupling the equations of motion for u_z and alternating magnetization $\vec{m} = (m_x, m_y, 0)$. Solving these equations produces the secular equation for coupled waves $(f^2 - f_{\text{AB}}^2)(f^2 - f_{\text{CB}}^2) = \xi f_H f_M f_{\text{AB}}^2$ [8, 9, 12–14]. Here, the terms in the left-hand side represent the dispersion laws for noninteracting AWs and a spin wave (SW); $\xi = B_2^2/(4\pi C M_0^2)$ is the parameter of their interaction, depending on magnetoelasticity constant B_2 [12]; $2\pi f_{\text{AB}} = kV$, $f_{\text{CB}}^2 = f_H(f_M + f_H)$, $f_H = \gamma(H + Dk^2)$, $f_M = \gamma 4\pi M_0$, M_0, D and $\gamma \approx 2.8$ MHz/Oe are the saturation magnetization, exchange rigidity, and gyromagnetic ratio, respectively. We find the MER conditions $(f, k) = (f_{\text{MER}}, k_{\text{MER}})$ from the phase match condition of AWs and SWs. The general solution for displacement and magnetization is written in the form $(u_z, m_{x,y}) = \sum(1, \alpha_{lx,y})A_l\exp(ik_l x)$, where $k_l = \pm|k_{1,2,3}|$ are the roots of the bicubic secular equation.

In all layers, the solutions of the equations of motion must satisfy the boundary conditions of the continuity of elastic displacements and stresses, along with additional conditions for magnetization at the FM layer boundaries (here $\partial m_{x,y}/\partial x = 0$). Solving the obtained equations provides all amplitude coefficients expressed through the alternating voltage supplied on electrodes *2* from an external source; we can also obtain the expression for the complex reflection coefficient from the transducer, $S_{11}(f, H)$.

Let us now consider the acoustic spin pumping. The SC density averaged over a wave period is written as $\vec{j}_s \propto g_r\theta^2\vec{n}$, where $\vec{n}$ is normal to the YIG lower surface; $\theta = \sqrt{\text{Im}\left[m_x^*(x_5)m_y(x_5)/M_0^2\right]}$ is the angle of the magnetization precession cone (see Fig. 1); and g_r is the characteristic parameter of s–d exchange interaction on the YIG/Pt interface [10]. An SC is detected because of the ISHE in Pt with characteristic angular parameter θ_{SH} [11]. Since θ_{SH} and g_r are characteristics of the spin detector (Pt) and YIG/Pt interface and can be considered as constants independent of the frequency, field, and layer thicknesses, the voltage across the Pt stripe is determined as $U_{\text{ISHE}} \propto (g_r\theta_{\text{SH}})\theta^2 \propto \theta^2$. The functional dependences of the ASP efficiency are therefore determined only by the angle of the precession cone, which is calculated using the results from the linear theory for components $m_{x,y}$.

Figure 2 shows the frequency dependences of U_{ISHE} (*a*, *c*) and $|S_{11}|$ (*b*, *d*) for constant magnetic field $H_0 = 744$ Oe and two irreversible structures (without YIG film *3*) with different thicknesses of film *5*. The material characteristics of the resonator layers correspond to the experiments described in [5]. The difference between frequencies f_{MER} and $f_{\text{FMR}} \equiv f_{\text{SW}}$ $(k = 0)$ is a consequence of allowing for nonuniform exchange; it is 30 MHz, which is comparable to magnetoelastic gap value $\sqrt{\xi f_H f_M}$ and is one order of magnitude greater than Δf_n. The considerable asymmetry of dependence $U_{\text{ISHE}}(f, H_0)$ with respect to f_{MER} (H_0)

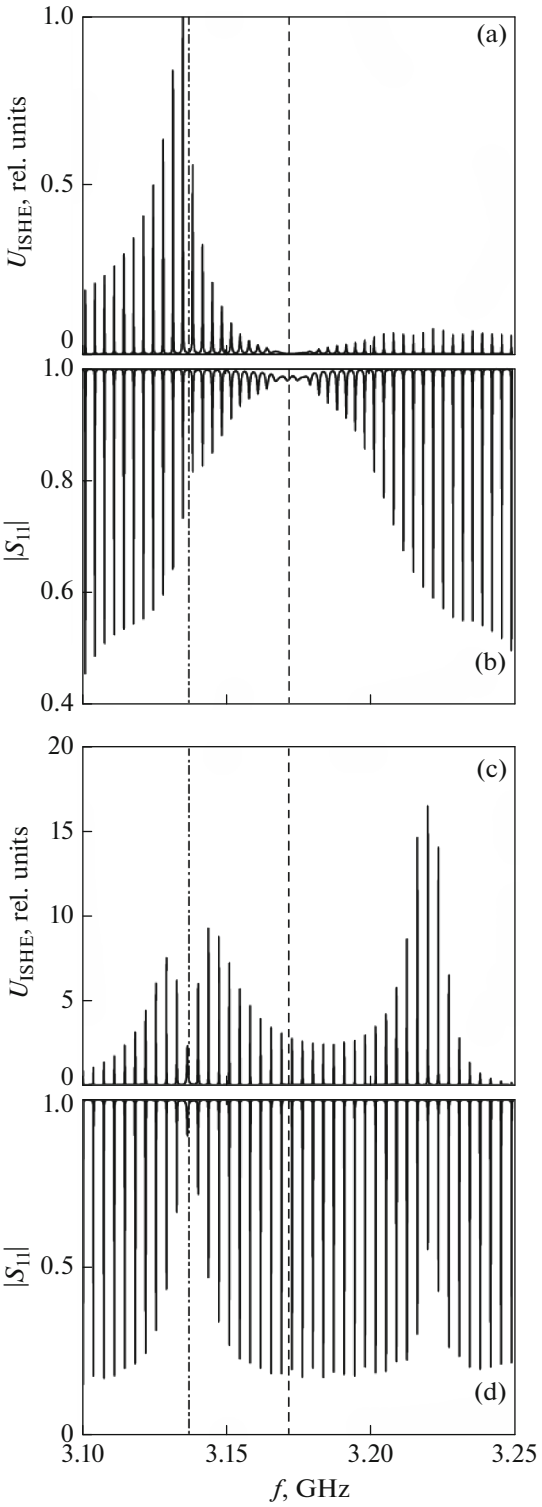

Fig. 2. Frequency dependences of (a, c) normalized constant voltage signal U_{ISHE} and (b, d) magnitude of reflection coefficient $|S_{11}|$ under a constant magnetic field with $H_0 = 744$ Oe and YIG film thicknesses (a, b) $s = 31$ μm and (c, d) $s = 0.4$ μm. The dashed lines correspond to frequency f_{MER}; the dashed-and-dotted lines, to frequency f_{FMR}.

(see Fig. 2a) is similar to the one observed earlier in our experiment. Frequency f_0 of the envelope maximum of $U_{ISHE}(f, H_0)$ is located slightly below frequency f_{FMR} (by approximately 1 MHz), which coincides with the results from other theoretical works (see, e.g., [14]). It is characteristic that the behavior of $|S_{11}(f, H_0)|$ (Fig. 2b) shows no qualitative difference in frequency detuning lower or higher than frequency f_{MER} (H_0). Fitting the calculated and experimental dependences of U_{ISHE} and $|S_{11}|$ on the frequency and magnetic field yields the characteristic constants $B_2 = 4 \times 10^6$ erg cm^{-3} and $D = 4.46 \times 10^9$ Oe cm^2. For magnetization, we obtain $4\pi M_0 = 955$ G, which is also typical for the doped YIG used in the experiment [5].

Analysis of the effect of FM film thickness s on the efficiency of spin pumping shows that reducing s from an initial value of 31 μm to ~0.2 μm raises the maximum of $U_{ISHE}(f_0, s)$ by more than one order of magnitude, and it is then observed to drop sharply. It should be noted that in the 0.15 μm $< s <$ 2–3 μm range of thicknesses, additional frequency regions appear where the maxima of $U_{ISHE}(f_k, s)$ are localized. With a nonuniform exciting effective magnetic field of an elastic nature, higher MWR modes (both even and odd) can be excited with efficiency comparable to that of the fundamental mode. An example of such excitation for the 0.4 μm YIG film is shown in Figs. 2c, 2d. The efficiency of MWR excitation at frequency $f_1 \approx 3.22$ GHz is even higher than that at frequencies in the vicinity of f_0.

CONCLUSIONS

A self-consistent theory was developed for calculating the spectra of a composite magnetoelectric resonator of bulk AWs, along with the direct voltage determined by two combined effects: acoustic spin pumping and ISHE. Qualitative and quantitative correlation between the calculated and experimental data was obtained.

FUNDING

This work was carried out within the framework of the state task and partially supported by the Russian Foundation for Basic Research, projects nos. 16-07-01210 and 17-07-01498.

REFERENCES

1. Uchida, K., An, T., Kajiwara, Y., et al., *Appl. Phys. Lett.*, 2011, vol. 99, no. 21, p. 212501.
2. Dreher, L., Weiler, M., Pernpeintner, M., et al., *Phys. Rev. B*, 2012, vol. 86, no. 13, p. 134415.
3. Weiler, M., Huebl, H., Goerg, F.S., et al., *Phys. Rev. Lett.*, 2012, vol. 108, no. 17, p. 17660.

4. Polzikova, N.I., Alekseev, S.G., Pyataikin, I.I., et al., *AIP Adv.*, 2016, vol. 6, no. 5, p. 056306.
5. Polzikova, N.I., Alekseev, S.G., Pyataikin, I.I., et al., *AIP Adv.*, 2018, vol. 8, no. 5, p. 056128.
6. Mansfeld, G.D., Alekseev, S.G., and Polzikova, N.I., *Proc. EEE Ultrasonics Symp.*, New York, 2008, p. 439.
7. Polzikova, N., Alekseev, S., Kotelyanskii, I., et al., *J. Appl. Phys.*, 2013, vol. 113, no. 17, p. 17C704.
8. Polzikova, N.I., Raevskii, A.O., and Goremykina, A.S., *J. Commun. Technol. Electron.*, 2013, vol. 58, no. 1, p. 87.
9. Polzikova, N.I., Alekseev, S.G., Luzanov, V.A., and Raevskiy, A.O., *Phys. Solid State*, 2018, vol. 60, no. 11, p. 2211.
10. Tserkovnyak, Y., Brataas, A., and Bauer, G.E.W., *Phys. Rev. Lett.*, 2002, vol. 88, no. 11, p. 117601.
11. Saitoh, E., Ueda, M., Miyajima, H., and Tatara, G., *Appl. Phys. Lett.*, 2006, vol. 88, no. 18, p. 182509.
12. Kittel, C., *Phys. Rev.*, 1958, vol. 110, no. 4, p. 836.
13. Tiersten, H.F., *J. Appl. Phys.*, 1965, vol. 36, no. 7, p. 2250.
14. Kamra, A., Keshtgar, H., Yan, P., and Bauer, G.E.W., *Phys. Rev. B*, 2015, vol. 91, no. 10, p. 104409.

Translated by N. Podymova